

Patient specific tracts-based analysis of diffusion compartment models: application to multiple sclerosis patients with acute optic neuritis

Olivier Commowick, Renaud Hédouin, Charlotte Laurent, Jean-Christophe Ferré

Synopsis (100 words)

Multiple sclerosis is a complex disease where voxel-based, group-based statistics of the brain microstructure have shown their limits in explaining patient evolution. This is first due to too simple diffusion models, mixing information. Voxel-based studies also lack knowledge on brain structural connectivity. Finally, group-based analysis does not describe well the specific patient status (a crucial point for clinicians). We propose an atlas-based framework, combined with advanced diffusion compartment models, for patient specific analysis of microstructural disease burden on major fiber bundles. We apply our framework to the analysis of optic radiations of MS patients with acute optic neuritis.

Short Synopsis (250 characters)

An atlas-based framework for patient specific analysis of microstructural disease burden along major fiber bundles. Application to multiple sclerosis patients suffering from acute optic neuritis showed different patterns of attacks on optic radiations.

1 Introduction

Multiple sclerosis (MS) is a complex disease [1] still not well understood. While MRI plays an important role in its diagnosis [2], there is still a clinical-radiological paradox [3, 4] in which handicap scores evolution is not correlated with MRI observations. This may come from the fact that the explored measures are not specific enough: all lesions are not equivalent depending on their position with respect to major fiber bundles and on the severity of the microstructural damage. To investigate this aspect, many studies have looked at diffusion MRI for its potential to reveal the brain microstructure [5]. However, diffusion MRI in MS has still not proven efficient yet for patient-specific follow-up. This comes first from the fact that current methodologies are often targeted at group analysis [6, 7, 8, 9]. Another reason is that although several methods have looked at along tract analysis [10, 11, 12], all methods are most often limited to simple models such as the tensor or to direction-based models that do not incorporate microstructure information. There is thus a need for patient, bundle specific measures of disease burden on directly interpretable parameters of the microstructure.

We propose a new framework for patient, bundle specific analysis of microstructural burden of neurodegenerative diseases. To do so, we propose an atlas-based approach to compute microstructural disease burden on major bundles with advanced diffusion compartment models (DCM) [13]. We evaluate this approach with a proof-of-concept analysis of optic radiations of MS patients with acute optic neuritis [14], showing different microstructural burden patterns depending on the patient.

2 Materials

Data from 22 control subjects and 6 MS patients with acute optic neuritis were acquired on a Siemens 3T Prisma scanner. For each subject, T1 and T2-weighted images (3D isotropic, 1 mm³) were acquired as well as diffusion images with a CUSP sequence [15] (6 b_0 , 60 directions with b -values in between 670 and 2000 s.mm⁻², 2x2x2 mm³ voxels). Data were preprocessed to remove distortion using a reversed phase encoding image [16] and DCM (three anisotropic tensors plus one free water and one isotropic restricted water compartments [13]) were estimated [17].

3 Methods

The overall pipeline of our method is composed of two parts: an offline part to compute a DCM enriched fiber atlas from controls (Fig. 1) performed once for all patients, and an online part performed for each patient (registration and comparison, Fig. 2).

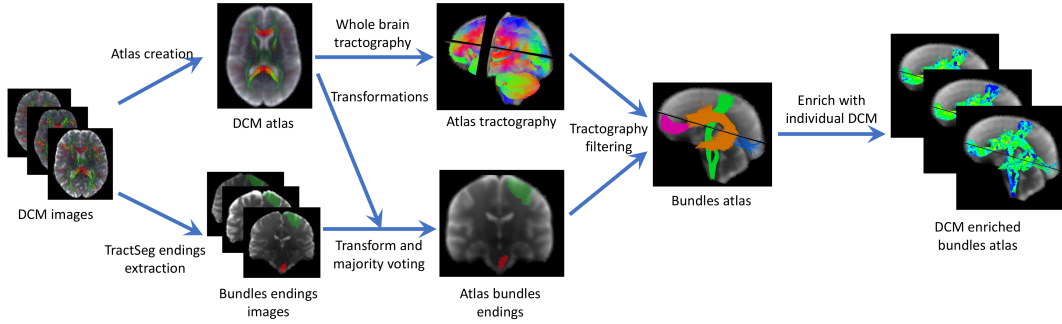


Figure 1: DCM enriched fiber atlas creation pipeline. From DCM images of controls, an atlas is created using tensor registration [18] and an unbiased atlas creation [19]. At the same time, TractSeg [20] is used to get bundles endings segmentations on each subject. These endings are then merged onto the atlas using majority voting. They are then used together with tractography [21] to get the major bundles on the atlas. Finally, the bundles are enriched with microstructural information along tracts extracted from DCM.

The offline part starts by the construction of a control DCM atlas [19]. Then, fibers are extracted over the whole atlas [21] and filtered using regions obtained through TractSeg [20] to get 72 different bundles. These bundles are then enriched with DCM information from each subject of the atlas. To do so, the DCM compartment most collinear to the fiber at a given point is selected and properties from it are extracted: mean diffusivity (MD), fractional anisotropy (FA), parallel and perpendicular diffusivities (d_{\parallel} , d_{\perp}); as well as water fractions of isotropic compartments fractions: free (FW) and isotropic restricted water (IRW) fractions.

The online part uses the control atlas as a reference for comparison. The patient DCM image is registered on the atlas [18]. Along the atlas bundles, information on patient microstructure is extracted from the patient DCM image and a statistical test of abnormality is computed at each point [22]. After correction for multiple comparisons [23], we compute disease burden scores $S_{b,p}$ for each bundle b and microstructure property p illustrating the abnormal fraction of the bundle:

$$S_{b,p} = 100 \frac{\sum_{i=1}^M \sum_{j=1}^{N_i} b_{i,j}}{\sum_{i=1}^M N_i} \quad (1)$$

with M number of fibers in bundle, N_i number of points in i -th fiber of bundle, $b_{i,j} = 1$ if the point j of fiber i in bundle b is abnormal (i.e. the statistical test performed on that point indicates a significant difference).

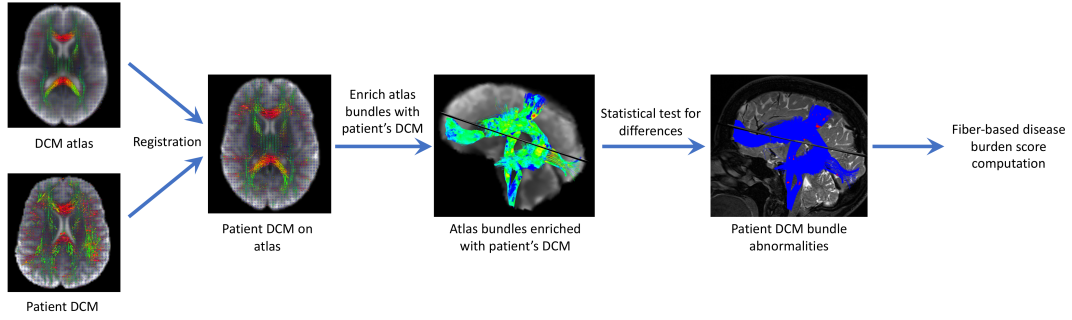


Figure 2: Fiber-specific disease burden computation for a patient DCM image. From the controls atlas and the DCM image of the patient, the patient is first registered on the atlas [18]. Then, the bundles of the atlas are enriched with microstructural information from the patient DCM image. Statistical tests [22] are performed at each fiber point to compare the patient’s along fiber microstructure to the controls. After correction for multiple comparisons [23], disease burden scores are computed for each bundle illustrating its level of abnormality for a given microstructure parameter.

4 Results

Fig. 3 presents results over the optic radiations of two patients suffering from acute optic neuritis related to MS, for two different microstructure parameters. It illustrates well the abnormalities that may be seen in those two patients, closely related to the presence of lesions. However the lesions seem to create different microstructural damage. This can be seen from Tables 1 and 2 where disease burden scores are higher for d_{\perp} and MD for patient 4, whereas it is higher for FW for patient 6. Moreover, at the time of acute optic neuritis, the higher disease scores for those two patients do not seem to be linked to the side of optic neuritis. No burden score is indeed above 10% on the right optic radiations.

Patient ID	Side	d_{\parallel}	d_{\perp}	MD	FA	FW	IRW
1	Left	0.63	2.86	2.62	3.56	0.29	1.51
2	Left	1.62	3.09	3.94	2.75	0.75	1.08
3	Left	2.14	1.77	3.02	2.51	2.33	1.94
4	Right	2.25	11.59	13.86	1.29	1.25	0.80
5	Left	0.90	0.75	0.71	0.91	3.58	2.15
6	Left	0.77	2.45	1.78	1.27	12.40	2.79

Table 1: Disease burden scores on left optic radiations for several along fiber microstructural properties: d_{\parallel} : parallel diffusivity, d_{\perp} : perpendicular diffusivity, MD: mean diffusivity, FA: fractional anisotropy, FW: free water fraction, IRW: isotropic restricted water fraction. Bold numbers denote burden scores above 10%. Side denotes which optic nerve suffers from optic neuritis.

5 Discussion and conclusion

We have proposed a new framework for the patient specific analysis of fiber bundles microstructural damage linked to a disease. We have derived the whole pipeline based on advanced compartmental models of diffusion, enabling the in-depth study of microstructural damage along major fiber tracts. Applied to MS patients suffering from acute optic neuritis, we have highlighted differences located primarily inside lesions but showing different microstructural differences depending on the patient, in line with the high variability of the disease. The code for this framework is available open-source [24]. Further works will study the influence of registration on the results, especially the need or not for advanced diffusion images registration; as well as other disease burden scores based on individual comparisons and their correlation with handicap scores.

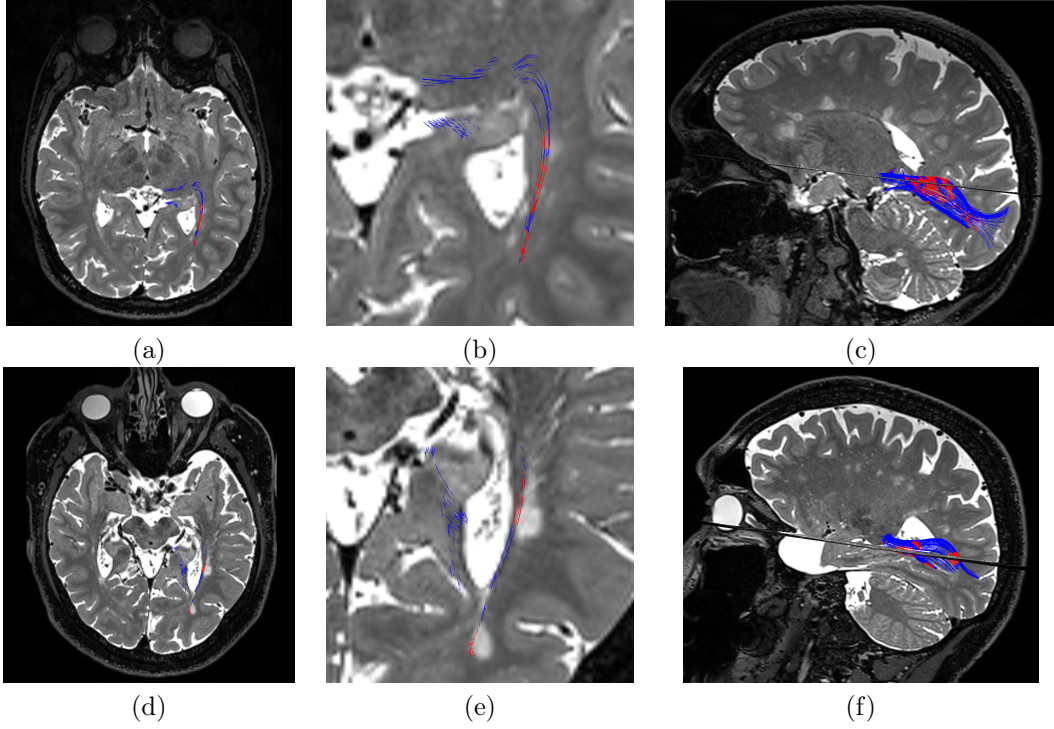


Figure 3: Results on two MS patients for two different microstructural properties. First line: patient 4 MD abnormalities along tracts. Second line: patient 6 FW abnormalities along tracts. (a,d): Axial view superimposing T2-weighted image and colored tracts, (b,e): zoom on the left optic radiation area, (c,f): 3D view of the T2-weighted image and colored optic radiations. On all images, red is a local significantly different abnormality, while blue is not.

Patient ID	Side	d_{\parallel}	d_{\perp}	MD	FA	FW	IRW
1	Left	1.38	0	0	0.08	0	0
2	Left	0	4.19	0	0.20	0	1.58
3	Left	0.09	0.01	0.02	0.47	1.09	0
4	Right	0	0.04	0	0.01	1.08	0.20
5	Left	0	0	0	0	0.06	0
6	Left	0	0	0	0.12	0.69	0

Table 2: Disease burden scores on right optic radiations for several along fiber microstructural properties: d_{\parallel} : parallel diffusivity, d_{\perp} : perpendicular diffusivity, MD: mean diffusivity, FA: fractional anisotropy, FW: free water fraction, IRW: isotropic restricted water fraction. No burden scores are above 10%. Side denotes which optic nerve suffers from optic neuritis.

Acknowledgments

This study was partially funded by grants from the VISIO foundation and the ARSEP (aide à la recherche sur la sclérose en plaques) foundation.

References

- [1] Fred D. Lublin, Stephen C. Reingold, Jeffrey A. Cohen, Gary R. Cutter, Per Soelberg Sorensen, Alan J. Thompson, Jerry S. Wolinsky, Laura J. Balcer, Brenda Banwell, Frederik Barkhof, Bruce Bebo, Peter A. Calabresi, Michel Clanet, Giancarlo Comi, Robert J. Fox, Mark S. Freedman, Andrew D. Goodman, Matilde Inglese, Ludwig Kappos, Bernd C. Kieseier, John A. Lincoln, Catherine Lubetzki, Aaron E. Miller, Xavier Montalban, Paul W. O'Connor, John Petkau, Carlo Pozzilli, Richard A. Rudick, Maria Pia Sormani, Olaf St??ve, Emmanuelle Waubant, and Chris H. Polman. Defining the clinical course of multiple sclerosis: The 2013 revisions. *Neurology*, 83(3):278–286, 2014.
- [2] Alan J Thompson, Brenda L Banwell, Frederik Barkhof, William M Carroll, Timothy Coetzee, Giancarlo Comi, Jorge Correale, Franz Fazekas, Massimo Filippi, Mark S Freedman, Kazuo Fujihara, Steven L Galetta, Hans Peter Hartung, Ludwig Kappos, Fred D Lublin, Ruth Ann Marrie, Aaron E Miller, David H Miller, Xavier Montalban, Ellen M Mowry, Per Soelberg Sorensen, Mar Tintoré, Anthony L Traboulsee, Maria Trojano, Bernard M J Uitdehaag, Sandra Vukusic, Emmanuelle Waubant, Brian G Weinshenker, Stephen C Reingold, and Jeffrey A Cohen. Diagnosis of multiple sclerosis: 2017 revisions of the McDonald criteria. *The Lancet Neurology*, 17(2):162–173, 2018.
- [3] Brian C. Healy, Guy J. Buckle, Eman N. Ali, Svetlana Egorova, Fariha Khalid, Shahamat Tauhid, Bonnie I. Glanz, Tanuja Chitnis, Charles R.G. Guttmann, Howard L. Weiner, and Rohit Bakshi. Characterizing clinical and MRI dissociation in patients with multiple sclerosis. *Journal of Neuroimaging*, 27(5):481–485, 2017.
- [4] F. Barkhof. The clinico-radiological paradox in multiple sclerosis revisited. *Current opinion in neurology*, 15(3):239–245, 2002.
- [5] M. Filippi, M. Cercignani, M. Inglese, and M.A. Horsfieldand G. Comi. Diffusion tensor magnetic resonance imaging in multiple sclerosis. *Neurology*, 56:304–311, 2001.
- [6] Natasha Lepore, Caroline A. Brun, Yi-Yu Chou, Ming-Chang Chiang, and et al. Generalized tensor-based morphometry of HIV/AIDS using multivariate statistics on deformation tensors. *IEEE Transactions on Medical Imaging*, 27(1):129–141, 2008.
- [7] M. Rovaris, A. Gass, R. Bammer, S.J.Hickman, O. Ciccarelli, D.H. Miller, and M. Filippi. Diffusion MRI in multiple sclerosis. *Neurology*, 65(10):1526–1532, 2005.
- [8] Brandon Whitcher, Jonathan J. Wisco, Nouchine Hadjikhani, and David S. Tuch. Statistical group comparison of diffusion tensors via multivariate hypothesis testing. *Magnetic Resonance in Medicine*, 57:1065–1074, 2007.
- [9] David A. Raffelt, J.-Donald Tournier, Robert E. Smith, David N. Vaughan, Graeme Jackson, Gerard R. Ridgway, and Alan Connelly. Investigating white matter fibre density and morphology using fixel-based analysis. *NeuroImage*, 144:58 – 73, 2017.
- [10] Stephen M. Smith, Mark Jenkinson, Heidi Johansen-Berg, Daniel Rueckert, Thomas E. Nichols, Clare E. Mackay, Kate E. Watkins, Olga Ciccarelli, M. Zaheer Cader, Paul M. Matthews, and Timothy E.J. Behrens. Tract-based spatial statistics: Voxelwise analysis of multi-subject diffusion data. *NeuroImage*, 31(4):1487 – 1505, 2006.
- [11] Maxime Chamberland, Mia Winter, Thomas Brice, Derek K. Jones, and Emma Tallantyre. Beyond lesion-load: Tractometry-based metrics for characterizing white matter lesions within fibre pathways. In *MICCAI 2020 - International Workshop on Computational Diffusion MRI*, 2020.

- [12] Maxime Chamberland, Sila Genc, Erika P. Raven, Greg D. Parker, Adam Cunningham, Joanne Doherty, Marianne van den Bree, Chantal M. W. Tax, and Derek K. Jones. Tractometry-based anomaly detection for single-subject white matter analysis. In *Medical Imaging with Deep Learning*, 2020.
- [13] E. Panagiotaki, T. Schneider, et al. Compartment models of the diffusion MR signal in brain white matter: a taxonomy and comparison. *Neuroimage*, 59(3):2241–2254, 2012.
- [14] N.R. Miller, N.J. Newman, V. Biousse, and J.B. Kerrison. *Walsh and Hoyt’s clinical neuro-ophthalmology*. Lippincott Williams & Wilkins, 2004.
- [15] Benoit Scherrer and Simon K. Warfield. Parametric representation of multiple white matter fascicles from cube and sphere diffusion MRI. *PLOS ONE*, 7(11):1–20, 11 2012.
- [16] R. Hédouin, O. Commowick, E. Bannier, B. Scherrer, M. Taquet, S. K. Warfield, and C. Barillot. Block-matching distortion correction of echo-planar images with opposite phase encoding directions. *IEEE Transactions on Medical Imaging*, 36(5):1106–1115, 2017.
- [17] Aymeric Stamm, Olivier Commowick, Simon K. Warfield, and S. Vantini. Comprehensive maximum likelihood estimation of diffusion compartment models towards reliable mapping of brain microstructure. In *Medical Image Computing and Computer-Assisted Intervention - MICCAI*, pages 622–630, 2016.
- [18] R.O. Suarez, O. Commowick, et al. Automated delineation of white matter fiber tracts with a multiple region-of-interest approach. *Neuroimage*, 59(4):3690–3700, February 2012.
- [19] Alexandre Guimond, Jean Meunier, and Jean-Philippe Thirion. Average brain models: A convergence study. *Computer Vision and Image Understanding*, 77(2):192 – 210, 2000.
- [20] Jakob Wasserthal, Peter Neher, and Klaus H. Maier-Hein. Tractseg - fast and accurate white matter tract segmentation. *NeuroImage*, 183:239 – 253, 2018.
- [21] D. Weinstein, G. Kindlmann, and E. Lundberg. Tensorlines: advection-diffusion based propagation through diffusion tensor fields. In *Proceedings Visualization ’99*, pages 249–530, 1999.
- [22] O. Commowick, A. Maarouf, et al. Diffusion MRI abnormalities detection with orientation distribution functions: A multiple sclerosis longitudinal study. *MedIA*, 22(1):114–123, May 2015.
- [23] Y Benjamini and Y Hochberg. Controlling the false discovery rate: A practical and powerful approach to multiple testing. *J. of the Royal Stat Society. Series B (Methodological)*, 57(1):289–300, 1995.
- [24] Inria Empenn team. Anima software - RRID:SCR_017072, <https://anima.irisa.fr>.